

Design of Safe Joint Module for Safe Robot Arm based on Passive and Active Compliance Methods

Hwi-Su Kim^{#1}, In-Moon Kim^{#2}, Jae-Bok Song^{#3}

[#]School of Mechanical Engineering, Korea University
Anam-dong, Seongbuk-gu, Seoul, Korea

¹fight704@korea.ac.kr, ²mydook@korea.ac.kr, ³jsong@korea.ac.kr

Abstract— In recent years, collision safety between humans and robots has drawn much attention because service robots are being increasingly used in human environments. Since various types of collisions can occur during robot operation, multiple safety methods should be required. To achieve the safety strategy based on both active and passive compliance methods, we propose a novel safe joint module composed of a speed reducer, a torque sensor, and a safety mechanism. The torque sensor embedded in the safe joint module can detect collision, and then the actuator is properly controlled to react against collision. However, if collision detection and reaction using a joint torque sensor fail due to the low bandwidth of a sensor, the safety mechanism composed of purely mechanical elements, such as springs and a cam follower, absorbs the collision force. With the proposed safety joint module, collision safety can be ensured by both active and passive compliance methods. Moreover, the external force applied to the robot arm can be measured for force control. High gear reduction and low backlash can be provided by the embedded harmonic drive. Several experiments on static and dynamic collisions show good performance of the safe joint module with active and passive compliance methods.

Keywords— Joint module, manipulator design, collision safety

I. INTRODUCTION

In recent years, humanoid robots and service robots have drawn much attention since service robots are increasingly used in human environments. Therefore, collision between humans and robots became one of the main issues, much research has been done to achieve collision safety [1-3].

Improving the safety of a robot arm can be achieved by either active or passive compliance. In the actively compliant arm, collision is detected by a sensor, and the manipulator stiffness can be decreased by appropriate control of a motor at each joint [4]. A passive compliance method consists of purely mechanical elements such as springs, link mechanisms and nonlinear stiffness system [5-7].

Previous approaches dealt with only one safety strategy, but it is often difficult to guarantee collision safety using only one approach. The active compliance approach has limited bandwidth since it involves sensing and actuation in response to a dynamic collision. Moreover, the scheme of sensing and actuation inevitably results in high cost, sensor noise, and possible malfunction. Also, if the safety mechanism is activated too frequently even against the low speed collision which does not cause harm to a human, it is not efficient for robot tasks. Since various types of collisions can occur during robot operation, multiple safety methods should be required to

prevent human injury.

In this research, we propose a novel safe joint module composed of a speed reducer, a torque sensor and a safety mechanism. The safe joint module can be applied to both active and passive compliance methods for collision safety. The embedded torque sensor can detect collision, and then the actuator is properly controlled to react against the collision. If the collision detection by the torque sensor fails due to the low bandwidth of the sensor, the safety mechanism absorbs the collision force.

Moreover, the proposed module can measure the external force applied to the robot arm for force control without an expensive force/torque sensor. High gear reduction and low backlash can be provided with the embedded harmonic drive.

The rest of the paper is organized as follows. The principle of operation and the structure of the safety mechanism are discussed in Section II. The structure and design procedure of the embedded torque sensor are presented in Section III. Section IV shows the structure of the proposed model. Various experimental results for both static and dynamic collisions are discussed in Section V. Finally, the conclusion and future work are presented in Section VI.

II. SAFETY MECHANISM

Nonlinear stiffness for both positioning accuracy and collision safety of a robot arm is difficult to generate using only linear springs. Therefore, in our previous research [5-6], nonlinear stiffness was realized by using the safety mechanism composed of a double-slider mechanism and linear springs, as shown in Fig. 1.

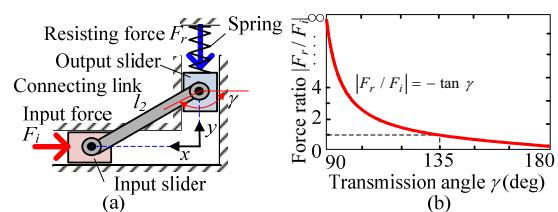


Fig. 1 Double-slider mechanism: (a) simplified model, and (b) force ratio vs. transmission angle.

This safety mechanism maintains very high stiffness up to a preset threshold torque for positioning accuracy, but provides very low stiffness above this threshold for collision safety. However, implementation of the safety mechanism for a robot arm requires a simple and compact design.

This paper presents a new safety mechanism shown in Fig. 2(a), which can be installed at the joint part of the robot arm more easily than our previous safety mechanism. The proposed safety mechanism consists of a cam, a cam follower and pre-compressed linear springs to achieve the nonlinear spring characteristic as shown in Fig. 2(b).

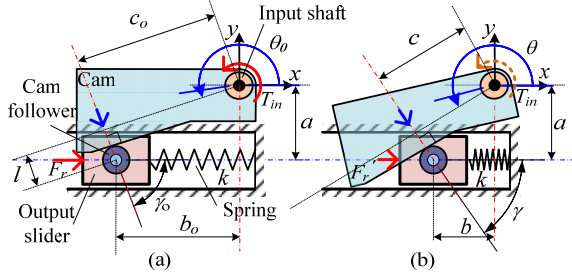


Fig. 2 Cam and Cam-follower mechanism for nonlinear stiffness: (a) zero configuration, and (b) general configuration.

From the equation of closure of the mechanism shown in Fig. 2, the relationship between T and F , which depends on the angle of inclination θ , can be given by

$$F = \frac{\cos(270^\circ - \theta)}{c} T \quad (1)$$

where the parameters c and θ are defined in Fig. 2. When the input torque T_{in} is exerted on the cam, the rotation of the cam applies an appropriate resisting force F_r to the output slider. Due to the spring force caused by spring compression, the output slider does not move, thereby generating an input torque large enough to move the slider. Once the input torque exceeds a preset threshold torque, the spring is rapidly compressed and stiffness of the safety mechanism abruptly drops. From Eq. (1), the threshold torque can be described by

$$T_{th} = \frac{c_o}{\cos(270^\circ - \theta_o)} k s_o \quad (2)$$

where subscript o represents the zero configuration, s_o is the spring compression at the zero configuration, and k is the spring constant. From Eq. (1) the equivalent stiffness, k_{eq} , seen from the input shaft can be obtained as a function of γ as follows:

$$k_{eq} = \frac{T_{in}}{\Delta\theta} = \frac{ks}{\theta - \theta_o} \frac{c}{\cos\gamma} \\ = \frac{k}{(\theta - \theta_o)\cos\gamma} \left\{ s_o + b_o - (a \tan\gamma) - \frac{l}{\cos\gamma} \right\} \times \left(\frac{a}{\cos\gamma} - l \tan\gamma \right) \quad (3)$$

where s is the spring compression, a , b and l are defined in Fig. 2, and γ and θ are related by $\gamma = 270^\circ - \theta$.

Fig. 3 shows an equivalent stiffness curve as a function of angular displacement of the input shaft when $k=5.7$ kN/m,

$a=14.5$ mm, $b_o=19.4$ mm, $c_o=22$ mm, $l=10.2$ mm, and $\theta_o=192^\circ$. The equivalent stiffness k_{eq} of this nonlinear system is kept very high for a small angular displacement of the input slider, but it quickly drops as the displacement increases. Hence the nonlinear stiffness system can be realized by the cam and cam-follower mechanism combined with a precompressed linear spring.

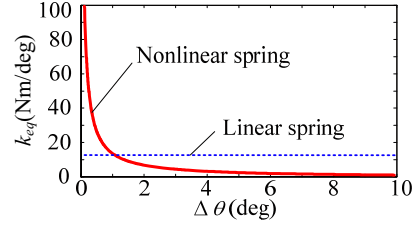


Fig. 3 Cam and Cam-follower mechanism for nonlinear stiffness: (a) simplified model, and (b) stiffness vs. rotation angle.

III. EMBEDDED TORQUE SENSOR

The joint torque sensor is integrated in the proposed safe joint module for collision detection and force measurement. When the embedded torque sensor in the safe joint module detects the collision that exceeds a certain threshold level, an actuator is properly controlled to react against this collision. In this section, the construction of an embedded torque sensor is presented.

A. Design of joint torque sensor

The structure of the joint torque sensor should be designed to have sufficient deformation in response to the external torque for precise measurement. However, large deformation has an adverse effect on positioning accuracy, so a tradeoff needs to be taken. In this research, the joint torque sensor has a hub-spoke type structure for the appropriate stiffness and high sensitivity. To search for the part sensitive to external torque, the FEM analysis on the structure of the joint torque sensor was conducted.

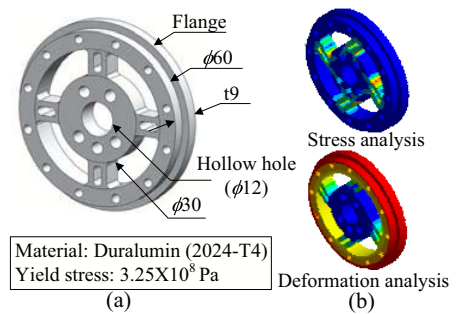


Fig. 4 Design of embedded joint torque sensor: (a) 3D modelling, and (b) stress and deformation analysis (FEM analysis).

Using the FEM analysis shown in Fig. 4(b), we could achieve the maximum allowable torque of 10 Nm in consideration of a safety factor of 3, and the rotational stiffness of 2.5×10^4 Nm/rad. This value should be larger than

the threshold torque of the safety mechanism to measure the external torque during the normal operation of the robot.

B. Torque sensing with Wheatstone bridge

The torque sensor consists of four strain gauges in a Wheatstone bridge configuration as shown in Fig. 5. Strain gauges bonded on the surfaces are deformed together with the sensing element of the torque sensor structure which is bended due to the external force.

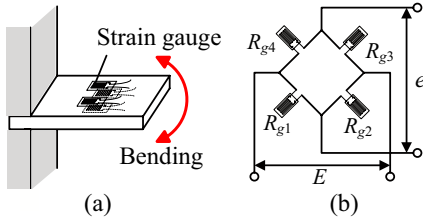


Fig. 5 Measurement of bending: (a) installation of strain gauges for torque measurement, and (b) full-bridge circuit.

The strain ε is given by

$$\varepsilon = \frac{4}{E \cdot K_s} e \quad (4)$$

where e is the output voltage, E is the applied voltage to the Wheatstone bridge, and K_s is the gauge factor. Since the relationship between ε and e is linear, torque can be calculated using the output voltage and the proportional factor from the experiments.

Strain gauges are attached to the sensitive region from the FEM analysis as shown in Fig. 6. The strain gauge wires are connected to the amplifier through the hollow shaft of the safe joint module. Furthermore, moment load is supported by the cross roller bearing.

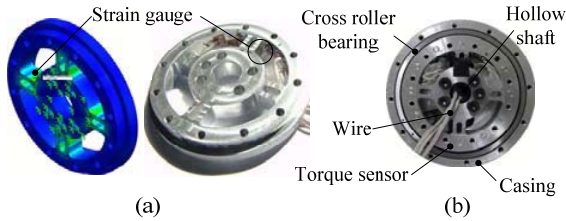


Fig. 6 Construction of embedded joint torque sensor: (a) Position for strain gauge and prototype, and (b) installation of torque sensor.

IV. CONSTRUCTION OF SAFE JOINT MODULE

The safe joint module composed of a gear reducer, a safety mechanism, a torque sensor, cross-roller bearings and a hollow shaft was constructed as shown in Fig. 7. For speed reduction, low backlash and lightweight design, a CSD type harmonic drive was used. The safety mechanism and torque sensor were designed in consideration of the installation at the safe joint module.

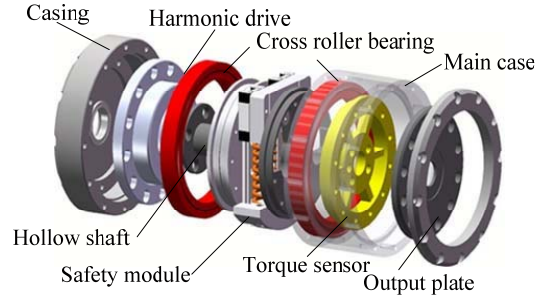


Fig. 7 Structure of proposed safe joint module.

Two cross roller bearings were installed to support the moment load, and the hollow shaft was used for cabling. The outer casing of the safe joint module was constructed with the aluminum alloy instead of steel to achieve lightweight design. A motor installed in the robot arm was connected with the safe joint module using a timing belt for power transmission.

In the safe joint module, external torque can be measured by the embedded torque sensor, since the cam plate fixed at the torque sensor does not move due to the holding force from spring compression during normal operation. When the external torque exceeds the threshold level, the actuator is controlled to react. If the collision detection fails due to the malfunction or low bandwidth of the sensor, the cam plate rotates since the generated force exceeds the sustaining force, and then the cam follower is forced to move on the LM guide to compress springs, as shown in Fig. 8. This cam movement reduces the stiffness of the safety mechanism, so the collision force can be absorbed. In this research, the threshold torque was set to 7.2 Nm.

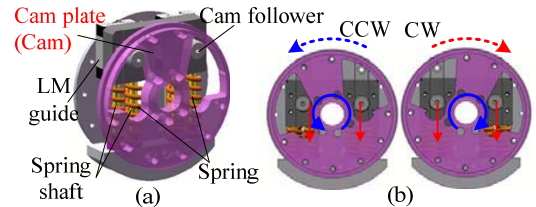


Fig. 8 Design of safety mechanism: (a) Structure of safety mechanism, and (b) operation after collision.

A prototype of the safe joint module was constructed to evaluate its performance, as shown in Fig 9. The specifications of the safe joint module are presented in Table I.

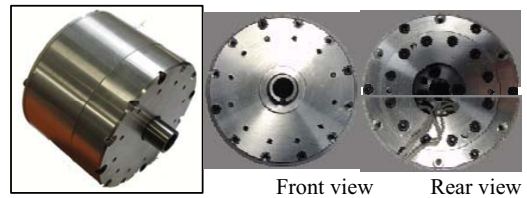


Fig. 9 Prototype of safe joint module.

TABLE I
SPECIFICATIONS OF SAFE JOINT MODULE

Specifications		
Weight	950 g	
Dimension	$\phi 86 \times 63$ mm	
Gear ratio	1 / 160	
Threshold torque	7.2 Nm	
Torque sensing	~ 10 Nm	
Component	Speed reducer	Harmonic drive (CSD20)
	Cross roller bearing	RA6008C

V. EXPERIMENTS USING SAFE JOINT MODULE

To verify the performance of the safe joint module when the manipulator collides with a human, various experimental results are presented in this section. Section A discusses performance (e.g., linearity and accuracy) of the embedded torque sensor. Section B shows results which verify nonlinear stiffness of the safe joint module. Section C discusses the collision safety of the manipulator with and without the safe joint module..

A. Performance test of embedded torque sensor

The experimental setup shown in Fig. 10 was designed to evaluate the developed embedded torque sensor. The torque sensor was connected to a commercial F/T sensor via the 1-DOF arm and flexible coupling. Angular contact bearings were used to eliminate the moment load except for the rotational direction.

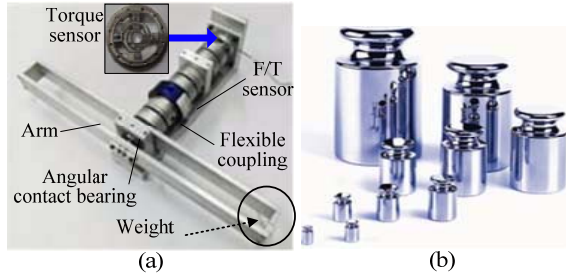


Fig. 10 Experimental setup for performance test of embedded torque sensor: (a) experimental setup, and (b) weight.

For evaluation of the linearity of the torque sensor, weights were applied to the 1-DOF arm to generate torque ranged from 0 to 12 Nm. Then, the output voltage from the torque sensor was recorded to verify correlation between the output voltage and the external torque. As shown in Fig. 11(a), linearity of the torque sensor was 98.2% using the least-square fit method. Fig. 11(b) shows the results of the comparison of the measured torque by the designed torque sensor with that by the F/T sensor when random torque was applied at the arm of the experimental setup.

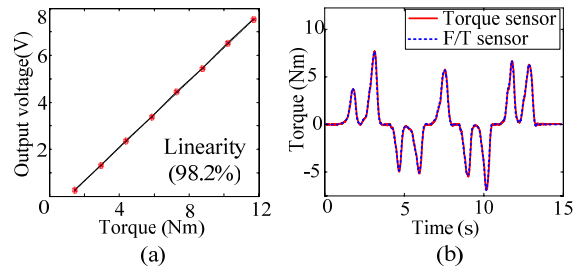


Fig. 11 Comparison between designed torque sensor and commercial F/T sensor: (a) linearity and torque coefficient, and (b) torque with random input.

B. Performance test of safety mechanism with static collision

The experimental setup shown in Fig. 12 was constructed for the evaluation of nonlinear stiffness of the safety mechanism. The safe joint module was installed at the 1-DOF robot arm which consists of a motor, link, and belt-pulley connection. The plate of the safe joint module integrated with the 1-DOF robot link was attached to the frame. The motor was connected to the input shaft of the safe joint module using a timing belt. Therefore, the motor torque can be transmitted to the robot link via the safety mechanism which was included in the safe joint module. To press the wall continuously after collision, the robot arm was commanded to reach the desired position, which was 20° inside the wall. When the experiments without the safe joint module were conducted, only a harmonic drive was used for speed reduction instead of the safe joint module.

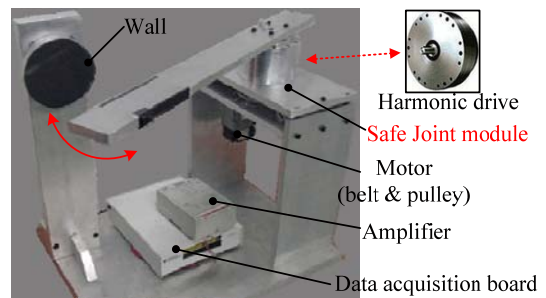


Fig. 12 Experimental setup for 1-DOF robot arm with and without safe joint module.

As shown in Fig. 13, the joint torque of the robot arm without the safe joint module increased up to 10 Nm at the wall due to high of the harmonic drive, which corresponds to the contact force between the robot arm and the wall. However, the joint torque of up to only 7.1 Nm was generated by the robot arm with the safe joint module, which was similar to the pre-determined threshold torque of 7.2 Nm, because excessive torque was absorbed by the safe joint module.

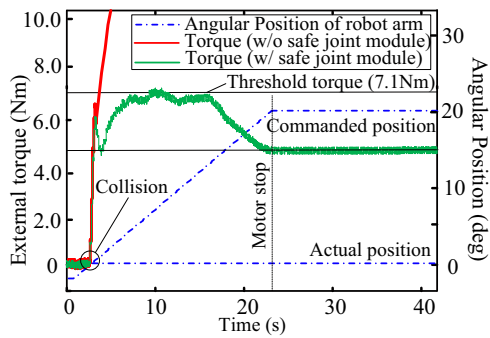


Fig. 13 Experimental results with static collision to verify nonlinear stiffness characteristic of proposed mechanism.

C. Safety test for dynamic collision

The experiments on dynamic collision were conducted to investigate the collision safety performance of the robot arm with and without the safe joint module. In this experiment, the end point of the robot arm collided at a constant velocity of 1.75 m/s. To achieve collision safety, the robot arm was programmed to stop when 6 Nm or higher torque was detected from collision. Experiments were conducted for the robot arm with and without the safe joint module.

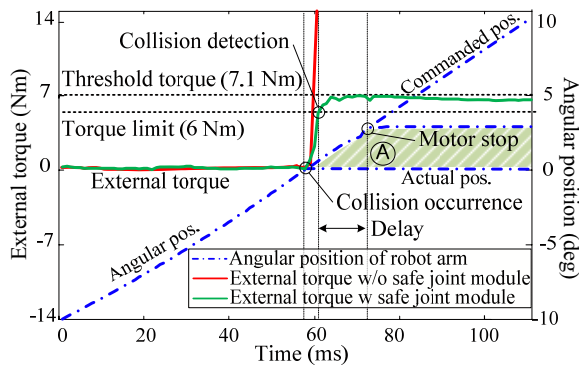


Fig. 14 Experimental results with dynamic collision with and without safe joint module.

Fig. 14 shows the experimental results when the robot arm collided with the wall at a constant velocity of 1.75 m/s. The collision force at the wall reached more than 10 Nm without the safe joint module. With the safe joint module, the operation of the robot arm stopped when the external torque of 6 Nm was measured by the embedded joint torque sensor.

When the robot arm was commanded to make an emergency stop in response to an external torque, a control delay usually occurs because of limited bandwidth due to sensing and actuation. At this time, the external torque increased continuously until the motor was stopped. In this research, however, the external torque was absorbed by the safety mechanism until the motor came to a complete stop as the stiffness of the safe joint module was abruptly dropped. The area A shown in Fig. 14 represents the safe region, which indicates that the safety mechanism was operated after the collision to absorb the torque generated by the motor, which

still ran even after the arm was stopped. Therefore, the maximum torque was limited to 7.1 Nm which was similar to the pre-determined threshold torque of 7.2 Nm.

VI. CONCLUSIONS

This paper proposed a safe joint module composed of a speed reducer, a torque sensor and a safety mechanism. With the proposed safety joint module, collision safety can be guaranteed by active and passive compliance methods. Therefore, reliable collision safety against various types of collisions can be achieved using a safe joint module. Based on our analysis and experiments, the following conclusions are drawn:

1. Collision safety based on the passive compliance method can be achieved, since the stiffness of the manipulator abruptly drops if the external torque induced by collision exceeds the pre-determined threshold torque.
2. Collision safety based on the active compliance method can be achieved, since a collision force can be detected by the embedded torque sensor, and the actuator can be properly controlled to react against collision.
3. The proposed module can measure the external force applied to the robot arm for force control without an expensive force/torque sensor.

ACKNOWLEDGMENT

This work was supported by the Project for Development of Manipulation Technology for Human-Robot Cooperation and by the Center for Autonomous Intelligent Manipulation under the Human Resources Development Program for Robot Specialists of Ministry of Knowledge Economy.

REFERENCES

- [1] M. Zinn, O. Khatib, B. Roth and J. K. Salisbury, "A new actuation approach for human-friendly robot design," *International Journal of Robotics Research*, vol. 23, no. 4/5, pp. 379-398, 2005.
- [2] G. Tonietti, R. Schiavi and A. Bicchi, "Design and control of a variable stiffness actuator for safe and fast physical human/robot interaction," *IEEE International Conference on Robotic and Automation*, pp. 528-533, 2005.
- [3] J. Echávarri, G. Carbone, J. L. Muñoz, M. Ceccarelli, "Safety Issues for Service Robots", *International Journal of Mechanics and Control*, vol. 8, no. 02, pp. 3-8, 2007.
- [4] S. Haddadin, A. Albu-Schaffer, A. De Luca and G. Hirzinger, "Collision detection and reaction: a contribution to safe physical human-robot interaction," *IEEE/RSJ International Conference on Intelligent Robots and Systems*, pp. 3356-3363, 2008.
- [5] H.-S. Kim, J.-J. Park, and J.-B., "Safety Joint mechanism using double slider mechanism and spring for humanoid robot arm," *IEEE-RAS International Conference on Humanoid Robots*, pp. 73-78, 2008. S. M. Metev and V. P. Veiko, *Laser Assisted Microtechnology*, 2nd ed., R. M. Osgood, Jr., Ed. Berlin, Germany: Springer-Verlag, 1998.
- [6] J.-J. Park, B.-S. Kim, J.-B. Song and H.-S. Kim, "Safe Link Mechanism based on Nonlinear Stiffness for Collision Safety," *Mech. Mach. Theory*, Vol. 43, No. 10, pp. 1332-1348, 2008. 10.
- [7] S. Kang and M. Kim, "Safe Arm Design for Service Robot," *Proc. of the International Conference on Control, Automation and System*, pp.88-95, 2002.